Australian Journal of Basic and Applied Sciences, 5(12): 937-945, 2011
ISSN 1991-8178

Analysis of Rolling Contact Fatigue Damage Initiation At The Wheel-Rail Interface

N.A. Akeel, Z. Sajuri and A.K. Ariffin

Department of Mechanical & Materials Engineering, Faculty of Engineering and Built Environment
Universiti Kebangsaan Malaysia, 43600 Bangi, Selangor, Malaysia.

Abstract: Rolling contact fatigue (RCF) results in damages on the railhead surface and wheel tread. The current paper presents the analysis of RCF damage initiation and stress distribution at the wheel-rail interface at different directions. A three-dimensional elastic frictional finite element model of the wheel-rail interaction is used to investigate the effect of the applied contact loading force at the straight, transition, and curved areas of the wheel tread and railhead surface. The interaction between the left and right wheels is considered. The interface exhibits small damage problems that are solved via the finite element method (FEM) software code ANSYS 11. The half-space assumption of the Hertz method is avoided by FEM. The real geometry and the boundary condition of the wheel-rail interface are accurately shown by the proposed simulation. The numerical results indicate the fatigue life and equivalent stress at the straight, transition, and curved areas of the rail track. Significant effect damages from the contact force on the wheel tread and the curve radius of rail track are observed at the interface.

Key words: Curved track; fatigue life; finite element method; wheel-rail.

INTRODUCTION

The railway track in Malaysia has shown the necessity of an efficient management of railway systems. The design is aimed toward reducing costs and increasing safety, as well as reliability, of the railway systems. The wheel-rail interface is one of the most crucial points that must be checked to determine the performance of a train and consider its safety. However, the calculation of the stress at the wheel-rail interface is dependent on the static and dynamic loading. The damage in this area is due to the repeated cyclic loading of the wheel. The damages that affect the mechanisms of fatigue are some of the concerns for the life prediction for a railway track. Fatigue causes abrupt fractures in the railhead and wheel tread. These failures may cause damage to rails because of the stress caused by the contact force as stated in the Hertz contact theory (Hosseini Tehrani, 2009).

The stress distribution and fatigue initiation at the wheel-rail interface are calculated by numerical and analytical methods. The problems that satisfied the assumptions in Hertz contact theory and some practical problems that do not meet the required assumptions in the aforementioned theory are elucidated in the current research. The interface is a small area compared with the body dimension and surface curvature of the wheel-rail contact region (Ringsberg, J.W. 2001; Liu, Y., 2006). A semi-analytical approach is developed for stress calculation using three-dimensional (3D) finite element analysis but the contact force is considered based on the Hertz theory. Fine meshing technique at the contact region is used to ensure an efficient and accurate computation. The stress response of the numerical analysis of the wheel rolling motion on running railhead surface is used for fatigue life prediction and the equivalent stress (von mises) criterion.

In the wheel-rail rolling contact problem, the interface is near the railhead surface and wheel tread. The finite element method (FEM) for contact analysis is used to solve the model of such problems (Sraml, M., 2003; Kyung Su Kim, 2005). The Hertz contact theory is used to calculate the stress response and fatigue damage problems. The principle stress-strain component in one direction is used for rolling contact fatigue analysis (Liu, Y., 2005). The two-dimensional (2D) finite element model is used to analyze their proposed model, and a multiaxial fatigue model is developed for bearing rolling contact fatigue analysis (Howell, M., 1995; Guo, Y.B., 2004; Fatemi, A., 1988). In the current research, a 3D simulation finite element model for wheel-rail rolling contact analysis is developed. However, the criterion for multi-axial fatigue of ductile material behavior is considered in the models. The influences of several parameters are evaluated, and conclusions based on the present results are obtained. The Goodman approach is used when the mean stress effects are considered. The method developed in the current study may be used for fatigue life design and service planning of a railroad.

Material Properties:

The material used is a used steel rail track provided by Permanent Way Division, KTMB. The chemical composition of the rail track material is examined, and the maximum composition of the material (Cr+Mo+Ni+Cu+V) is limited to be less than 0.35% (Table 1). The mechanical properties of the rail track material are shown in Table 2. These properties are compared with the standard requirement for rail track

Corresponding Author: N.A. Akeel, Department of Mechanical & Materials Engineering, Faculty of Engineering and Built Environment Universiti Kebangsaan Malaysia, 43600 Bangi, Selangor, Malaysia.
E-mail: nuri2008@eng.ukm.my

material set by KTMB. The tensile properties of the tested rail material complied with the standard property requirements. Bending strength is not included as one of the parameters to be considered in the standard property requirements for rail track material set by KTMB. However, this property is one of the most important parameters in determining crack propagation resistance or fracture resistance of the rail material under Mode I loading.

Table 1: Chemical compositions of rail track material.

C	Mn	Si	P	S	Cr+Mo+Ni+Cu+V
0.60-0.80	0.83-1.30	0.10-0.50	<0.05	<0.05	<0.35

Table 2: Mechanical properties of the rail material.

Yield stress (MPa)	Tensile strength (MPa)	Young's modulus (GPa)	Poisson's ratio
825	923	200	0.3

Finite Element Method (FEM):

A complete FEM model composed of two wheels and a piece of two rails track is used to analyze the stress distribution at different curve radii. The simulation is a set of the element size and the quasi-static loads on the wheel created with a library of ANSYS 11. Force is applied on the wheel which has contact with the rail. Here, the rail and the wheel tread are defined as two separate profiles. The shape of wheel and rail profiles generated with a standard mathematical model is described by several keypoints. The Goodman approach in ANSYS 11 via the FEM is used in all simulations to predict the mean stress effects. The detail drawing the wheel and rail contact model is presented in the previous work (Akeel, N.A., 2011). The 3D geometric model of the wheel is generated by revolving the 3D curves that describe the profile of the wheel tread. The rail model is created by extruding railhead profile curves a distance of 600 mm, which is the distance between the sleepers. The two sets of curves for the new wheels and rails created by the solid model are shown in Figure 1.

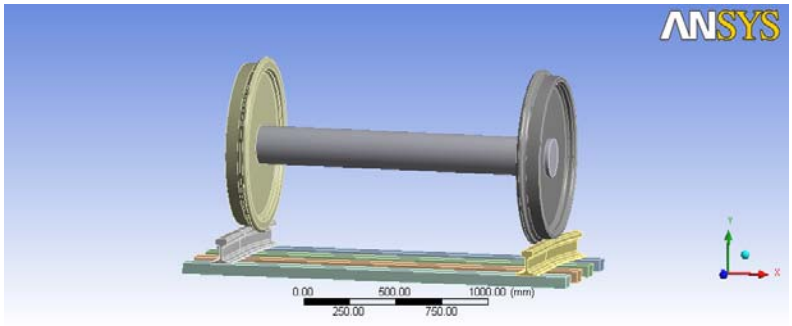

Fig. 1: Solid model of wheel/rail contact.

Fine mesh is used in the finite element of the solid model (Figure 2). To predict a reasonable model configuration, the wheel is spatially oriented relative to the rail according to the quasi-static state calculated by FEM. A geometric shape, domains, a material model, a value for the coefficient of friction, and knowledge about the contact forces are required to produce a model of the wheel-rail interaction (Sladkowski, A., 2005). The material model is based on the stress-strain curves obtained in the previous work (Akeel, N.A., 2011).

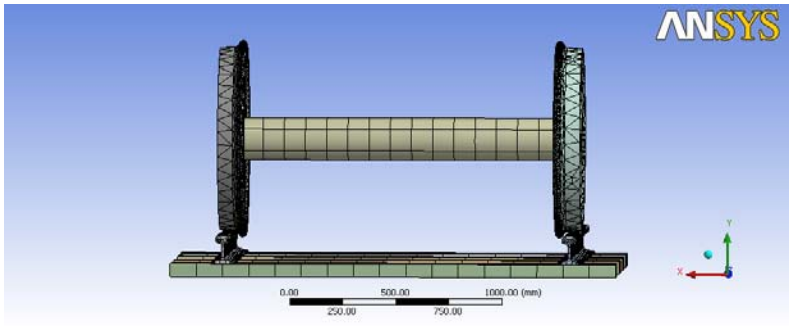

Fig. 2: Finite element modeling of wheel/rail contact.

Condition Of Wheel-Rail Interface:

The different rail track position (straight, transition, and curved areas) are simulated in the model of a railway track in Malaysia. The radius of the curved area and the different degree of curvature with every radius of the curve are shown in Table 3. However, at the transition area with θ= 25°, the right wheel is higher than the left wheel during motion when the rail track condition shifts from the straight to the curved area (Figure 3). Therefore, the transition starts from a straight area and changes to the curved area. The curved area is defined as a shift from the transition area to a straight area as shown Figure 4.

Table 3: Relationship with curve radius and Degree of curvature.

Curve Radius (m)	Degree of curvature
100	12°
200	10°
300	8°
400	6°
500	4°
600	4°
700	4°
800	4°
900	4°
1000	4°

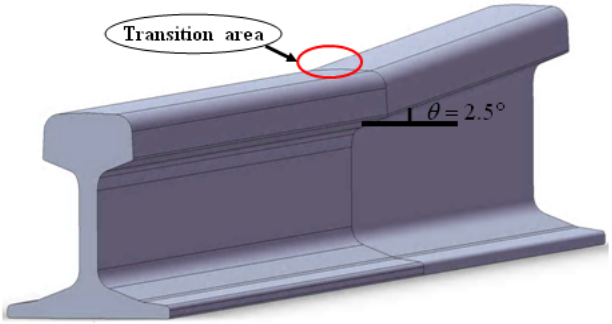

Fig. 3: Rail track at transition area.

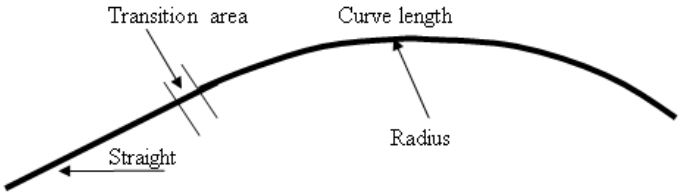

Fig. 4: Crack position on straight, transition and curve radius of rail track.

Numerical Analysis Method:

Crack Initiation Life Damage:

The fatigue crack initiation life prediction and stress distribution under different vertical loading is calculated using the wheel-rail RCF model. The contact force is assumed at the maximum value based on the over loading of passengers on the train. The design load of the model is applied on the wheel tread on the running surface of railhead (Makoto, A.K.A.M.A., 2007). Damage tolerance on the wheel-rail interface is defined by the following equation:

$$FP = \left(\sigma^{\max}\right)\frac{\Delta\varepsilon}{2} + J\Delta\tau\Delta\gamma \tag{1}$$

The constant J is the maximum stress normal to the crack plane, $\Delta\varepsilon$ is the strain range normal to the crack plane, $\Delta\tau$ is the shear stress range on the crack plane, $\Delta\gamma$ is the shear strain range on the crack plane, and $FP_{\max}$ is the fatigue parameter value defined as the crack plane. The load is chosen as the contact force loading on the wheel and rail contact areas. The equation for the fatigue crack initiation for the crack plane is as follows (Kapoor, A., 1994):

$$FP\max = \left(\left\langle \sigma^{\max} \right\rangle \frac{\Delta\varepsilon}{2} + J\Delta\tau\Delta\gamma\right)_{\max}$$
$$= \frac{(\sigma')^2}{E}\left(2N_f\right)^{2b} + \sigma'_f\,\varepsilon'_f\left(2N_f\right)b + c \tag{2}$$

The crack initiation life is calculated to determine the number of cycles of fatigue life as follows:

$$N_f = \varepsilon_c / \Delta\varepsilon_r \tag{3}$$

where ε_c is a material constant determined experimentally, and $\Delta\varepsilon_r$ is the equivalent ratcheting strain per cycle and calculated as

$$\Delta\varepsilon_r\sqrt{\left(\Delta\bar{\varepsilon}\right) + \left(\Delta\gamma/\sqrt{3}\right)^2} \tag{4}$$

$\Delta\bar{\varepsilon}$ and $\Delta\bar{\gamma}$ are calculated as the incremental normal and shear strain acting on the crack plane per load cycle. The load is the force applied on the wheel tread on the running surface of the railhead at the contact region. Therefore, this equivalent ratcheting strain per cycle can be used to investigate the crack initiation corresponding to the material response elucidated through the FEM analysis.

Curve Radius of Rail Track:

The curve radius of the railway track is defined as the radius of the approximating circle. The curve radius is enlarged so the formula for the curve radius *R* for a horizontal curve can be determined by obtaining the intended design velocity *V*, the coefficient of friction, and the allowed superelevation on the curve radius of rail track.

$$R = \frac{\upsilon^2}{g\left(e + f_s\right)} \tag{5}$$

Using this radius, practitioners can determine the degree of curve to check whether it falls within acceptable standards. The degree of curve, D_a, can be computed through the following formula:

$$\%R = \frac{1746}{D_a}\% \tag{6}$$

where D_a is the degree of curve along the horizontal curve radius.

The horizontal curve is found at locations where two roadways intersect, providing a gradual transition between the two paths. The intersection point of the two roads is defined as the Point of Tangent Intersection **(*PI*)**. The location of the starting point of the curve is defined as the Point of Curve **(*PC*)**, whereas that of the end point is defined as the Point of Tangent **(*PT*)**. Both *PC* and *PT* are at a distance *T* from *PI*, where *T* is defined as the Tangent Length and can be calculated by determining the central angle of the curve, in degrees. This angle is equal to the supplement of the interior angle between the two road tangents.

$$T = R\tan\left(\frac{\Delta}{2}\right) \tag{7}$$

where *T* is the tangent length (in length units), Δ is the central angle of the curve (in degrees), and *R* is the curve radius (in length units).

The distance between *PI* and the vertex of the curve can be easily calculated using the property of right triangles with *T* and *R*. Considering this distance and subtracting the curve radius *R*, the external distance *E*, the smallest distance between the curve and *PI*, can be obtained.

$$E = R\left(\frac{1}{\cos\left(\frac{\Delta}{2}\right)} - 1\right) \tag{8}$$

where E is the external distance (in length units). Similarly, the middle ordinate M can be found and is the maximum distance between the line drawn between PC, PT, and the curve. This distance falls along the line between the vertex of the curve and PI.

$$M = R\left(1-\cos\left(\frac{\Delta}{2}\right)\right) \tag{9}$$

where M is the middle ordinate (in length units), and L is the curve length that can be determined using the formula for semicircle length.

$$L = \frac{R\Delta\pi}{180} \tag{10}$$

Similarly, the geometric formula for cord length can be used to calculate C, which represents the cord length for this curve.

$$C = 2R\sin\left(\frac{\Delta}{2}\right) \tag{11}$$

RESULTS AND DISCUSSION

The wheel-rail contact model predicts that the maximum value of the von mises stress decreases, in contrast to that of the fatigue life (Figure 5). However, the rolling contact damage life initiation increases at the straight area, in contrast to its trends at the transition and curved areas in the wheel-rail contact model. The contour plots the von mises stresses of static and dynamic loading on the wheel tread and railhead surface. The results describe the deformation of the stress distribution at the transition and curved areas of wheel-rail interface as the results of the different curve radii of the rail track as shown in Figures 6–11.

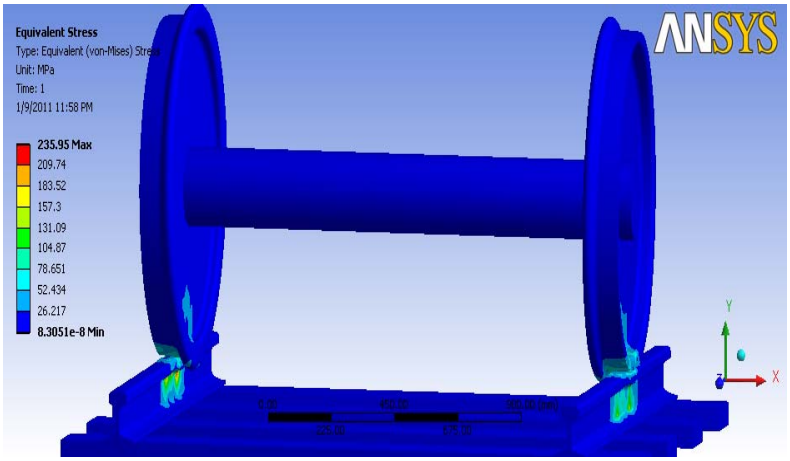

Fig. 5: Equivalent stresses (von mises) at straight track.

The maximum rolling contact damage at the wheel-rail interface occurs at the corner gauge of the rail track. The fatigue life of the wheel-rail interface increases as the radius curve increases. However, the value of the contact loading force increases, in contrast to the fatigue life initiation, at the wheel-rail interface. The effect of curve radius and angles in wheel-rail contact model on the maximum fatigue life initiation at the right rail track is plotted in Figure 12.

The maximum value of the von mises stress of the wheel-rail interface decreases with different contact loading forces from 80 KN to 120 KN and as the sharp radius curve of the rail track increases. The distribution of the von mises stress in the right rail is higher than that in the left rail with the curve radius of rail track. The effect of the different curve radii and angles in wheel-rail contact model on the maximum von mises stress in the right rail is plotted in Figure 13.

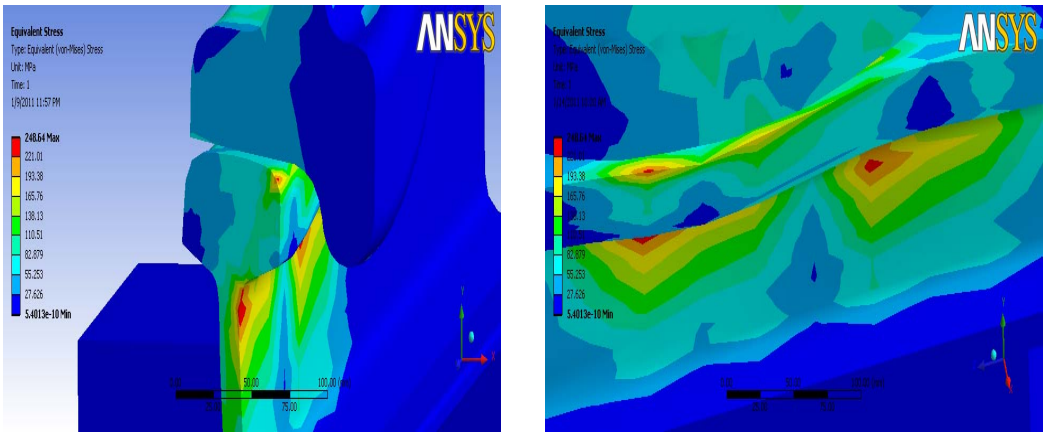

(a) Front section (b) Left section

Fig. 6: Equivalent stresses (von mises) at transition area.

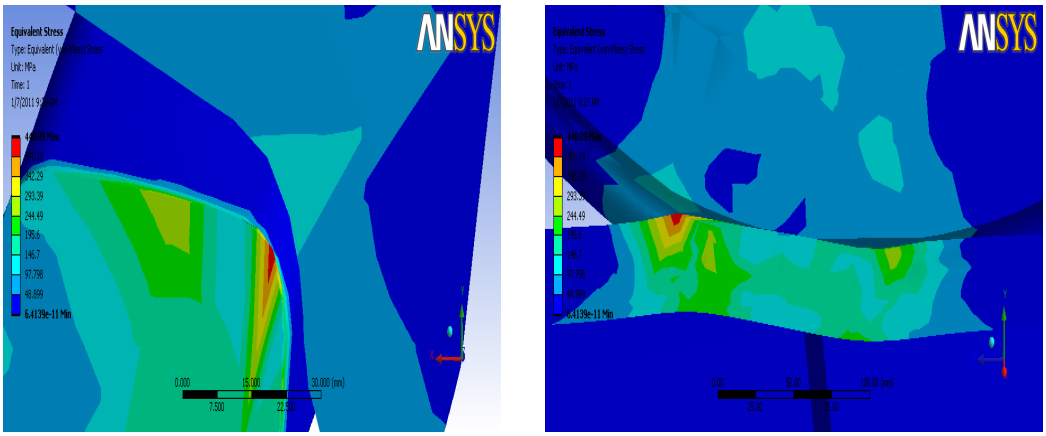

(a) Front section (b) Left section

Fig. 7: Equivalent stresses (von mises) at curve radius track 100mm.

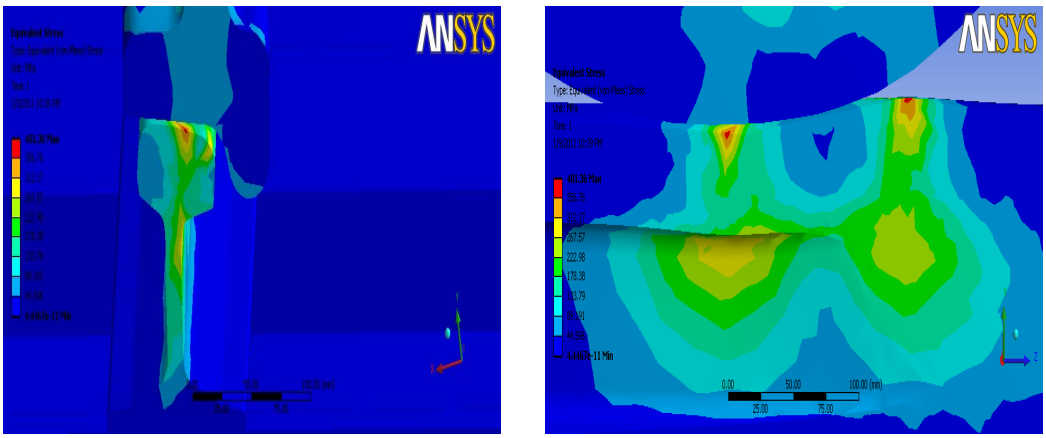

(a) Front section (b) Left section

Fig. 8: Equivalent stresses (von mises) at curve radius track 200mm.

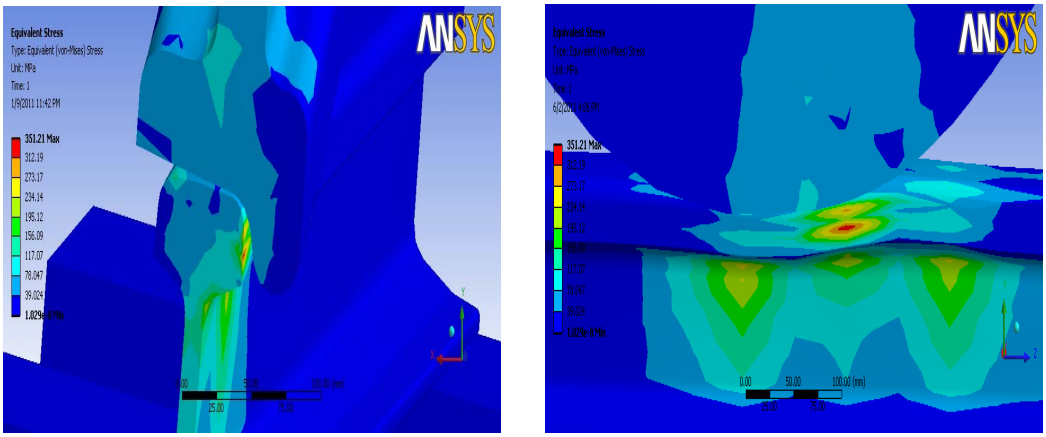

(a) Front section (b) Left section

Fig. 9: Equivalent stresses (von mises) at curve radius track 300mm.

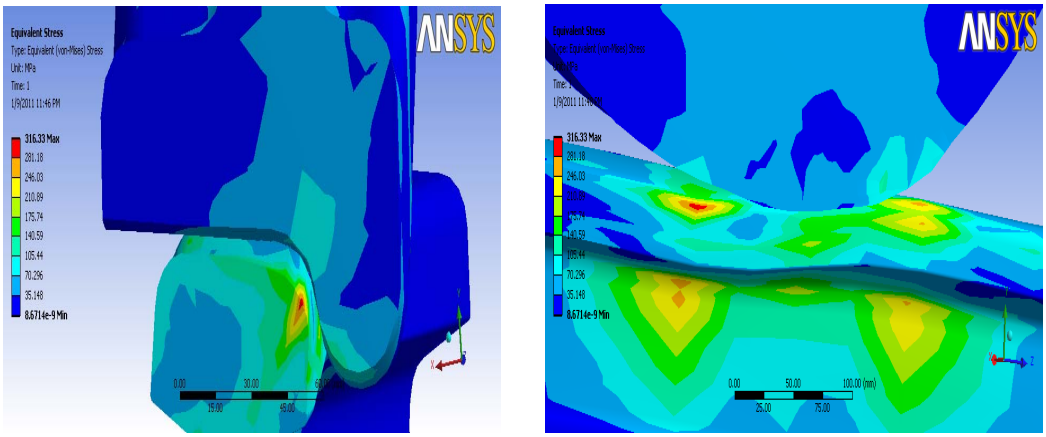

(a) Front section (b) Left section

Fig, 10: Equivalent stresses (von mises) at curve radius track 400mm.

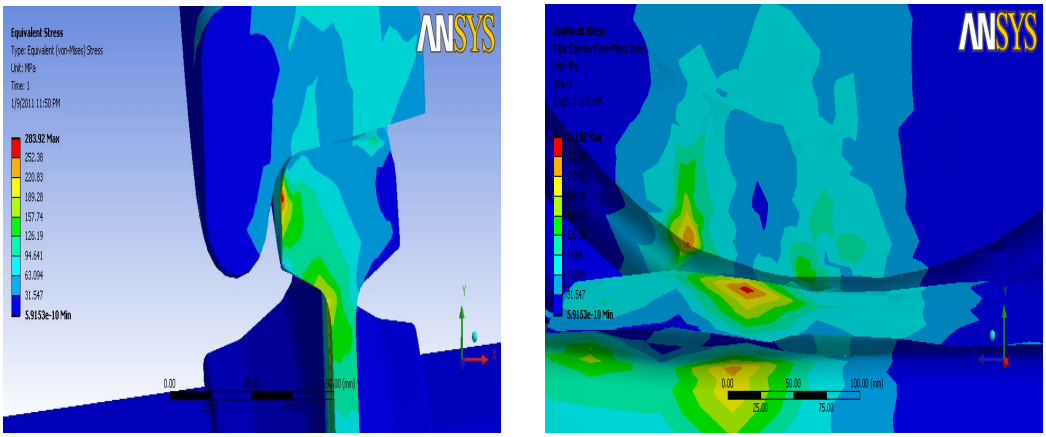

(a) Front section (b) Left section

Fig. 11: Equivalent stresses (von mises) at curve radius track 500mm.

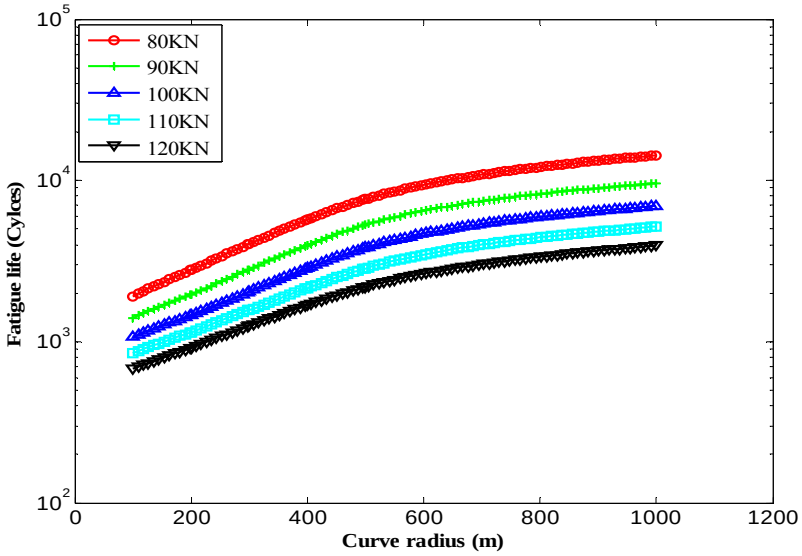

Fig. 12: The fatigue life prediction of different area.

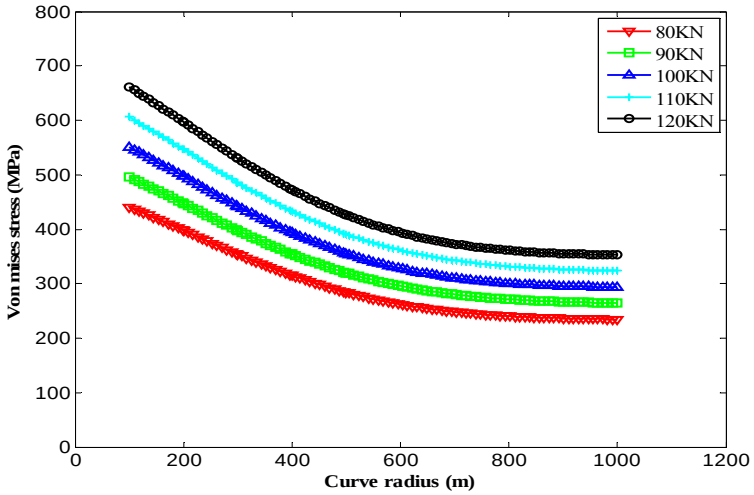

Fig. 13: The equivalent stresses (von mises) at different area.

Table 4: The results of stress and fatigue life at straight and transition area.

Load (KN)	Von mises stress (MPa)		Fatigue life (cycle)	
	Straight area	Transition area	Straight area	Transition area
80	235	248	14314	11964
90	265	279	9604	8169
100	294	310	6934	5898
110	324	341	5165	4393
120	353	372	3947	3357

The fatigue life and von mises stress in wheel-rail contact model at the straight and transition areas of the rail track are shown in Table 4. However, the fatigue life increases at the straight area in contrast to its behavior at the transition area. The von mises stress in the wheel-rail contact model increases at the transition area in contrast to its behavior at the straight area of the rail track. The difference in the contact loading force and the angle of transition area is approximately θ =2.5. However, given that the straight area is a flat surface, thus, θ =0. Therefore, the maximum values of von mises stress at the transition area at the right rail track changes from the straight to the curved area.

Conclusion:

The effect of the von mises stress and the fatigue damage life initiation is demonstrated by the wheel-rail contact model. The results of the investigations in the current study can be summarized as follows:

1. An increasing contact loading force and decreasing curve radius results in more damage in the wheel-rail interface.
2. The von mises stress decreases at the straight area in the wheel-rail contact model compared with those at the transition and curved areas of the rail track.
3. The maximum value of the von mises stress is 660 MPa at the wheel-rail interface with an approximately 100 m curve radius as a result from an applied force load of approximately 120 KN.
4. The effect of fatigue damage life initiation increases at the straight area but decreases at the transition and curved areas in the wheel-rail contact model.
5. The maximum value of fatigue life prediction at the straight area is approximately 14314 cycles.

ACKNOWLEDGMENTS

The authors would like to thank Keretapi Tanah Melayu Berhad (KTMB) for supplying the rail track materials and to Ministry of Science, Technology and Innovation (MOSTI) for sponsoring this work.

REFERENCES

Akeel, N.A., M.A. Aziman, Zainuddin Sajuri, Ahmad Kamal Ariffin, A.W. Ikhsan, 2011. Identification of Damages and Stress Analysis of Rail/Wheel Rolling Contact Region. Key Engineering Materials, pp: 462-463.

Fatemi, A., D.F. Socie, 1988. Multiaxial fatigue damage including out-of-phase loading. Fatigue Fract Eng Mater Struct., 11: 149-65.

Guo, Y.B., M.E. Barkey, 2004. Modeling of rolling contact fatigue for hard-machined components with process induced residual stress. Int. J. Fatigue, 26(6): 605-13.

Hosseini Tehrani, P., M. Saket, 2009. Fatigue crack initiation life prediction of railroad, Journal of Physics: Conference Series 181. 012038, doi:10.1088/1742-6596/181/1/012038.

Howell, M., G.T. Hahn, C.A. Rubin, D.L. McDowell, 1995. Finite element analysis of rolling contact for nonlinear kinematic hardening bearing steel. ASME J Tribol., 117: 729-36.

http://www.wikibooks.org/Fundamentals of Transportation/ Horizontal Curves. on 26 May 2010.

Kapoor, A., 1994. "A re-evaluation of the life to rupture of ductile metals by cyclic plastic strain", Fatigue and Fracture of Engineering Materials and Structures, 17: 201-219.

Kyung Su Kim, Dong In Cho, Jae Wook Ahn, Seung Bok Choi, 2005. An Experimental Study on Fatigue Crack Propagation under Cyclic Loading with Multiple Overloads. Key Engineering Materials, 297-300, pp: 2495-2500.

Liu, Y., B. Stratman, S. Mahadevan, 2006. Fatigue crack initiation life prediction of railroad wheels. Int J Fatigue, 28(7): 747-56.

Liu, Y., S. Mahadevan, 2005. Multiaxial high-cycle fatigue criterion and life prediction for metals. Int J Fatigue, 7(7): 790-800.

Makoto, A.K.A.M.A., 2007. "Development of Finite Element Model for Analysis of Rolling Contact Fatigue Cracks in Wheel/Rail Systems". Quarterly Report of RTRI, 48(1): 8-14.

Ringsberg, J.W., 2001. Life Prediction of Rolling Contact Fatigue Crack Initiation, Int. J. Fatigue, 23: 575-586.

Sladkowski, A., M. Sitarz, 2005. Analysis of wheel-rail interaction using FE Software, Wear, 258: 1217-1223.

Sraml, M., J. Flasker, I. Potrc, 2003. Numerical procedure for predicting the rolling contact fatigue crack initiation. Int J Fatigue, 25(7): 585-95.